PHASE SPACE COATING IN SYNCHROTRONS: SOME APPLICATIONS*

C. M. Bhat# Fermilab, Batavia, IL 60510, U.S.A.

Abstract

Use of barrier buckets in synchrotron storage rings has opened new ways for beam stacking. Here we present some recent results from the operational experience of "longitudinal phase-space coating" [1] technique at the Fermilab Recycler for beam stacking, its usefulness to map the incoherent synchrotron tune of beam particles in a barrier bucket and its application to produce a clean hollow beam in longitudinal phase space.

LONGITUDINAL PHASE-SPACE COATING

The Recycler Ring (RR) [2] is used as the main antiproton repository for the Tevatron proton-antiproton collider program at Fermilab since 2004. For the best performance of the collider one requires high brightness pbar bunches which are created in the RR. The amount of pbars that can be stacked prior to the transfer to the Tevatron is limited by available phase space area in the RR, stochastic as well as electron cooling rate, beam

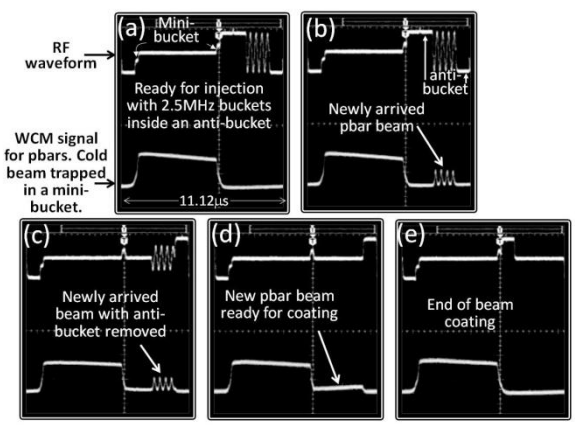

Figure 1: Scope pictures of various steps involved in pbar stacking in the Recycler using LPSC technique.

instability related to the high brightness and how efficiently beam is stacked by multiple transfers of newly produced antiprotons from the Pbar source. Consequently, one needs a robust and a fast stacking method with minimum emittance growth during stacking. In recent years two different techniques out of many presented in ref. 3 are pursued: morph-merging [4] and longitudinal phase-space coating (LPSC) [1]. ("phase-space coating" and the "LPSC" are used as synonyms here.) In the former method the cold pbar stack prior to the new transfer is likely to be disturbed and may become quite inefficient if the stack prior to the transfer is not cold enough. While in the second method the cooled beam is undisturbed throughout the process and also adopts some features of morph-merging.

The rf manipulation steps involved in morph-merging is explained in ref. 5. The general principle of the LPSC scheme is explained in ref. 1 and the various rf manipulation steps are shown in Fig. 1. A major portion of the cold stack is always captured in a mini-bucket and untouched during stacking as shown in Fig 1(a). When the new beam is about to be added, a small portion of the cold stack (not captured in the mini-bucket) will mix with the in-coming beam and coated on the beam in the mini-bucket. As the beam is cooled, more and more beam particles from the coated region will be trapped in the mini-bucket.

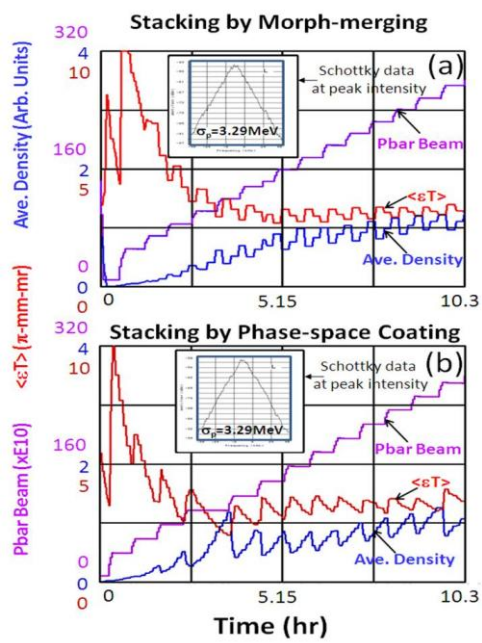

Figure 2: Comparison between stacking by morph-merging and LPSC during normal operation in the RR.

We have studied both the methods in detail in operation up to a stack intensity of ~4×10^{12}pbar in RR. Figure 2 shows measured average transverse emittance(<εT>), average beam brightness (blue curve) and pbar beam intensity for a stacked beam intensity up to 2.7×10^{12}. Each step in intensity indicates a new set of pbar transfer. The longitudinal Schottky spectra (insets in Fig. 2(a) & (b)) after merging the last set of transfers are also shown for comparison. In both cases the stochastic cooling as well as e-cooling were turned on during stacking. Consequently, the core of the cold beam (with synchrotron period in the range of several seconds) was

* Operated by Fermi Research Alliance, LLC under Contract No. DE-AC02-07CH11359 with the United States Department of Energy
#cbhat@fnal.gov

disturbed very little even though there was no mini-bucket to hold beam-core in the case of morph-merging scheme. As a result of this, operationally we find little difference between these two techniques.

MEASUREMENT OF INCOHERENT SPECTRUM USING LPSC

Mapping of the synchrotron frequency spectrum of particles in a standard rf bucket with a sinusoidal rf wave had been done before [6]. The LPSC method of beam stacking provides an elegant method to measure/map the synchrotron tune of beam particles in barrier buckets.

The incoherent synchrotron frequency f_s of beam particles inside a rectangular barrier bucket is given by,

$$\frac{1}{f_s} = 2\frac{T_2}{|\eta|}\frac{\beta^2 E_S}{\left|\tilde{\Delta E}\right|} + 4\frac{\left|\tilde{\Delta E}\right|}{eV_{rf}}T_S \text{ with } \tilde{\Delta E} = \sqrt{\frac{eV_{rf}}{T_S}\frac{\tilde{T}_1}{}\frac{2\beta^2 E_S}{|\eta|}}$$

where, e, η, E_S, $\tilde{\Delta E}$, $\tilde{T}_1, T_2$ and T_S are electronic charge, synchrotron slip factor (-0.0085), synchronous energy of RR (8.9 GeV), energy off-set of the particle from E_S, penetration depth of the particle into the rf barrier, pulse gap and revolution period of the synchronous particle (11.12 μs), respectively. Figure 3 presents a schematic of a rectangular barrier bucket with mini-bucket of half height $\tilde{\Delta E}$ and with definition of various parameters used in the above equation.

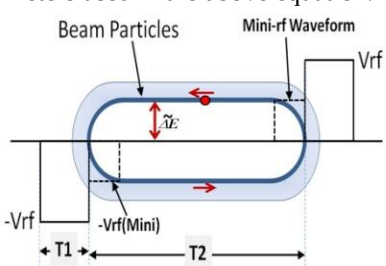

Figure 3: A schematic of the rf waveforms and hollow beam.

Experimental Method:

A barrier bucket with pulse height of V_{rf} =1.84 kV, pulse width T_1=0.9 μs and T_2 =5.9 μs is chosen here as the main bucket to map the synchrotron frequency spectrum. Then a mini-bucket of half bucket height = $\tilde{\Delta E}$ is grown inside the main bucket. Using the proton beam the empty mini-bucket was coated following the same steps as shown in Figs 1, thus creating a long bunch with a hole in the center. The separatrix of the mini-bucket acts as the boundary between the empty region and the coating. A wall current monitor (WCM) beam signal fed to a RTD720 digitizer scope, a 1.76GHz Schottky detector at a 19500th harmonic and wall current monitor signal fed to Agilent 89441A 2.65GHz VSA (with a frequency span of 0-4Hz, centered at the RR revolution frequency (VSA generates instantaneous complex spectra by doing FFT of the captured transient WCM signals) are used to measure line-charge distribution, particle Schottky spectrum and synchrotron spectrum of the beam, respectively.

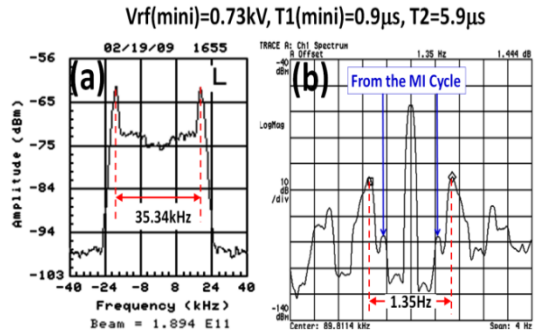

Figure 4: Typical (a) Schottky and (b) synchrotron spectra from VSA measurement of beam particles coated on the mini-bucket seperatrix.

Results and Data Analysis

Figure 4 shows Schottky and synchrotron frequency spectra of the beam particles corresponding to V_{rf}(mini)= 0.73 kV, T_1(mini)=0.9 μs and $\tilde{\Delta E}$ =11.1 MeV after coating on an empty bucket as shown in Fig. 3. In this case the synchrotron oscillation frequency of the beam particles sitting in the separatix of mini-bucket is 0.5×1.35 Hz=0.67±0.6 Hz, which is essentially the measured frequency of the particles in the inner edge of the spectrum as indicated in Fig. 4(b).

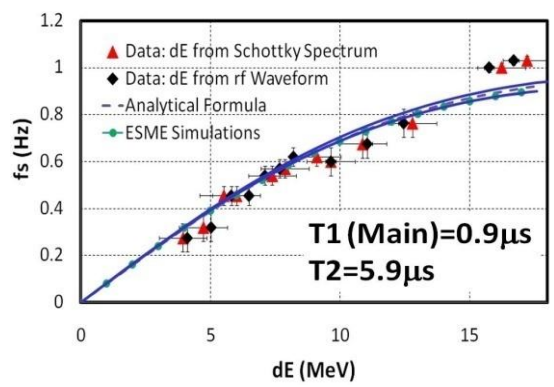

Figure. 5: Measured and calculated synchrotron frequency as a function of $\tilde{\Delta E}$ of beam particles in a RR barrier bucket with V_{rf} =1.84 kV, T_1=0.9 μs and T_2 =5.9 μs. The solid lines encompass uncertainties from the rf pulse height and pulse shape for analytically calculated f_s (dashed line). Results from ESME tracking are also shown for comparison.

The RR and the Fermilab Main Injector (MI) are located in the same underground tunnel and some cross

talk is expected. During these measurements we had multiple MI acceleration cycles at about 0.46 Hz. Consequently, the RR beam spectrum was complex and had more lines than that comes from the coated beam alone. The first harmonic lines corresponding to the MI cycle are also in Fig. 4(b) for illustration. At certain values of $\tilde{\Delta E}$, the MI cycles interfere with the beam particle spectrum resulting in large errors in the measurements.

The measured synchrotron frequency as a function of $\tilde{\Delta E}$ is shown in Fig. 5 along with analytical predictions and simulations using ESME [7]. The $\tilde{\Delta E}$ in each case is measured 1) by using known rf voltage of the mini-bucket 2) measuring the frequency difference between "horns" in the Schottky spectrum shown in Fig. 4 (a). The uncertainties in the data points are mainly coming from rf voltage calibration and/or establishing the inner rising edge of the Schottky and the synchrotron frequency spectra.

HOLLOW BEAM & ITS SIMULATIONS

During each of the measurements mentioned above a hollow bunch is created. However, the hole in the longitudinal phase space is maintained by means of mini-buckets. In the absence of any external cooling, no

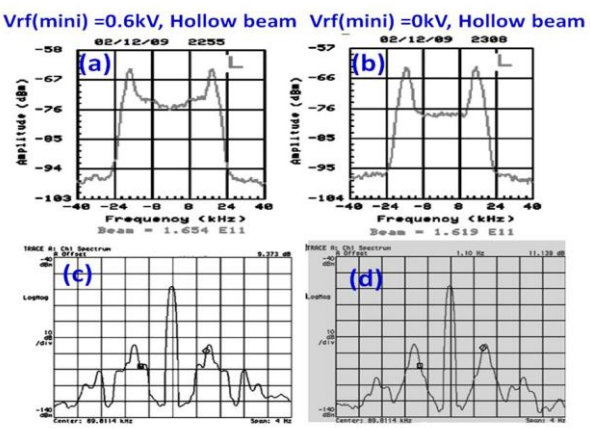

Figure 6: (a) Schottky, (c) synchrotron spectra are similar to one shown in Fig. 4 but for Vrf= 0.6 kV and $\tilde{\Delta E}$ =10.1MeV. The beam spectra (b) and (d) for the hollow beam without mini-bucket .

particles can fall into the mini-bucket. A hollow beam of interest is created by removing the mini-barrier bucket. Figure 6 shows beam spectrum of a hollow beam with mini-bucket and after adiabatic removal of the mini-bucket. We certainly observe some leakage of beam particles into the hollow region. This is manily because of non-adiabaticity of the rf manipulation while removing the mini-bucket. No degradation in hollow beam is seen even after a long time (of the order of hours).

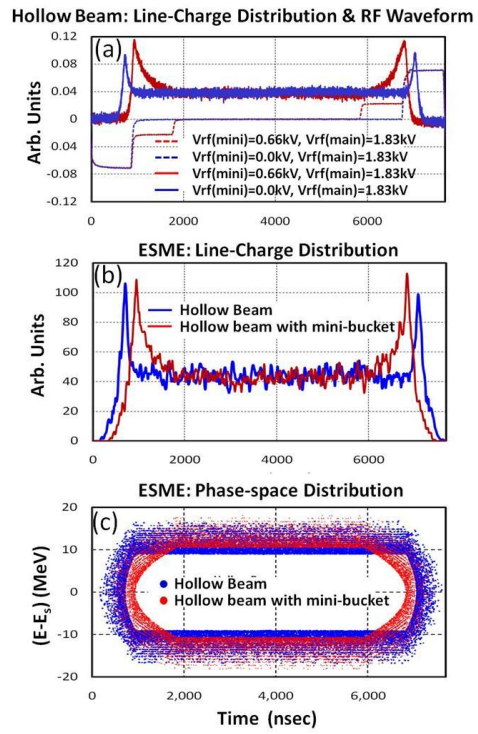

Figure 7: (a) Measured line-charge distribution, (b) ESME prediction of line-charge distribution and (c) predicted longitudinal phase-space distribution of the hollow bunch corresponding to the data shown in Fig.6.

Figures 7 (a) and (b) show measured and ESME predicted line-charge distributions for the hollow beam with and without the mini-buckets. The corresponding beam particle distribution in the longitudinal phase-space is shown in Fig. 7(c). We see rather good qualitative agreement in the predicted and the measured line-charge distributions.

The hollow beam of the type explained here may be of very high interest from the point of view of studying varieties of distribution functions and studying beam physics. At this time, hollow beams are of purely academic interest.

The author would like to thank D. Wildman and J. Crisp for their help in early VSA measurements, Cons Gattuso for his involvement in testing LPSC scheme in the RR operation and special thanks are due to the MCR crew.

REFERENCES

[1] C. M. Bhat, EPAC2008 (2008), p 307.
[2] G. Jackson, Fermilab-TM-1991.
[3] C. M. Bhat, FERMILAB-CONF-06-102-AD.
[4] P. Joireman and B. Chase (unpublished 2007).
[5] C. M. Bhat, FERMILAB-FN-0916-AD (2011).
[6] H. Huang et. al.,Phys.Rev.E48-4678(1993).
[7] J. A. MacLachlan, HEACC'98,184, (1998), http://www-ap.fnal.gov/ESME/es2009_4